

# Very Massive Stars in High-Redshift Galaxies

Mark Dijkstra<sup>1\*</sup> and J. Stuart B. Wyithe<sup>1†</sup>

<sup>1</sup>*School of Physics, University of Melbourne, Parkville, Victoria, 3010, Australia*

3 December 2018

## ABSTRACT

A significant fraction of Ly $\alpha$  emitting galaxies (LAEs) at  $z \geq 5.7$  have rest-frame equivalent widths (EW) greater than  $\sim 100\text{\AA}$ . However only a small fraction of the Ly $\alpha$  flux produced by a galaxy is transmitted through the IGM, which implies intrinsic Ly $\alpha$  EWs that are in excess of the maximum allowed for a population-II stellar population having a Salpeter mass function. In this paper we study characteristics of the sources powering Ly $\alpha$  emission in high redshift galaxies. We propose a simple model for Ly $\alpha$  emitters in which galaxies undergo a burst of very massive star formation that results in a large intrinsic EW, followed by a phase of population-II star formation with a lower EW. We confront this model with a range of high redshift observations and find that the model is able to simultaneously describe the following eight properties of the high redshift galaxy population with plausible values for parameters like the efficiency and duration of star formation: i-iv) the UV and Ly $\alpha$  luminosity functions of LAEs at  $z=5.7$  and  $6.5$ , v-vi) the mean and variance of the EW distribution of Ly $\alpha$  selected galaxies at  $z=5.7$ , vii) the EW distribution of i-drop galaxies at  $z\sim 6$ , and viii) the observed correlation of stellar age with EW. Our modeling suggests that the observed anomalously large intrinsic equivalent widths require a burst of very massive star formation lasting no more than a few to ten percent of the galaxies star forming lifetime. This very massive star formation may indicate the presence of population-III star formation in a few per cent of i-drop galaxies, and in about half of the Ly $\alpha$  selected galaxies.

**Key words:** cosmology–theory–galaxies–high redshift

## 1 INTRODUCTION

Narrow band searches for redshifted Ly $\alpha$  lines have discovered a large number of Ly $\alpha$  emitting galaxies with redshifts between  $z = 4.5$  and  $z = 7.0$  (e.g. Hu & McMahon 1996; Hu et al. 2002; Malhotra & Rhoads 2002; Kodaira et al. 2003; Dawson et al. 2004; Hu et al. 2004; Stanway et al. 2004; Taniguchi et al. 2005; Westra et al. 2006; Kashikawa et al. 2006; Shimasaku et al. 2006; Iye et al. 2006; Stanway et al. 2007; Tapken et al. 2007). The Ly $\alpha$  line emitted by these galaxies is very prominent, often being the only observed feature. The prominence of the Ly $\alpha$  line is quantified by its equivalent width (EW), defined as the total flux of the Ly $\alpha$  line,  $F_{\text{Ly}\alpha}$  divided by the flux density of the continuum at  $1216\text{\AA}$ :  $\text{EW} \equiv F_{\text{Ly}\alpha}/f_{1216}$ . Throughout this paper we refer to the rest-frame EW of the Ly $\alpha$  line (which a factor of  $(1+z)$  lower than the EW in the observers frame).

Approximately 50% of Ly $\alpha$  emitters (hereafter LAEs) at  $z = 4.5$  and  $z = 5.7$  have lines with  $\text{EW} \sim 100 - 500\text{\AA}$

(Dawson et al. 2004; Hu et al. 2004; Shimasaku et al. 2006). For comparison, theoretical studies conclude that the maximum EW which can be produced by a conventional population of stars is  $200-300\text{\AA}$ . Moreover, this maximum EW can only be produced during the first few million years of a starburst, while at later times the luminous phase of Ly $\alpha$  EW gradually fades (Charlot & Fall 1993; Malhotra & Rhoads 2002). Therefore, observed EWs lie near the upper envelope of values allowed by a normal stellar population.

The quoted value for the upper envelope of  $\text{EW} \sim 200 - 300\text{\AA}$  corresponds to the emitted Ly $\alpha$  flux. However not all Ly $\alpha$  photons are transmitted through the IGM, and we expect some attenuation. Within the framework of a Cold Dark Matter cosmology, gas surrounding galaxies is significantly overdense, and possesses an infall velocity relative to the mean IGM (Barkana 2004). As a net result, the IGM surrounding high redshift galaxies is significantly opaque to Ly $\alpha$  photons. Indeed it can be shown that for reasonable model assumptions, only  $\sim 10 - 30\%$  of all Ly $\alpha$  photons are transmitted through the IGM (Dijkstra et al. 2007). As a result, the intrinsic Ly $\alpha$  EW emitted by high redshift LAEs is systematically larger than observed. Indeed, this observation suggests that a significant fraction of LAEs at  $z \geq 4.5$

\* E-mail: [dijkstra@physics.unimelb.edu.au](mailto:dijkstra@physics.unimelb.edu.au)

† E-mail: [swyithe@physics.unimelb.edu.au](mailto:swyithe@physics.unimelb.edu.au)

have intrinsic EWs that are much larger than can possibly be produced by a conventional population of young stars.

One possible origin for this large EW population is provided by active galactic nuclei (AGN), which can have much larger EWs due to their harder spectra (e.g. Charlou & Fall 1993). However, large EW LAEs are not AGN for several reasons: (1) the Ly $\alpha$  lines are too narrow (Dawson et al. 2004) (2) these objects typically lack high-ionisation state UV emission lines, which are symptomatic of AGN activity (Dawson et al. 2004), and (3) deep X-Ray observations of 101 Ly $\alpha$  emitters by Wang et al. (2004, also see Malhotra et al. 2003, Lai et al, 2007) revealed no X-ray emission neither from any individual source, nor from their stacked X-Ray images.

Several recent papers have investigated the stellar content of high-redshift LAEs by comparing stellar synthesis models with the observed broad band colors (Finkelstein et al. 2007). These comparisons are often aided by deep IRAC observations on *Spitzer* (Lai et al. 2007; Pirzkal et al. 2007). In this paper we take a different approach. Instead of focusing on individual galaxies, our goal is to provide a simple model that describes the population of Ly $\alpha$  emitting galaxies as a whole. This population is described by the rest-frame ultraviolet (UV) and Ly $\alpha$  luminosity functions (LFs) at  $z = 5.7$  and  $z = 6.5$ , and the Ly $\alpha$  EW distribution at  $z = 5.7$  (Shimasaku et al. 2006; Kashikawa et al. 2006). The sample of high-redshift LAEs is becoming large enough that meaningful constraints can now be placed on simple models of galaxy formation.

The outline of this paper is as follows: In § 2–§ 5 we describe our models. In § 6 we discuss our results, and compare with results from stellar synthesis models, before presenting our conclusions in § 7. The parameters for the background cosmology used throughout this paper are  $\Omega_m = 0.24$ ,  $\Omega_\Lambda = 0.76$ ,  $\Omega_b = 0.044$ ,  $h = 0.73$  and  $\sigma_8 = 0.74$  (Spergel et al. 2007).

## 2 THE MODEL

Dijkstra et al. (2007b) found that the observed Ly $\alpha$  LFs at  $z = 5.7$  and  $z = 6.5$  are well described by a model in which the Ly $\alpha$  luminosity of a galaxy increases in proportion to the mass of its host dark matter  $M_{\text{tot}}$ . One can constrain quantities related to the star formation efficiency from such a model (also see Mao et al. 2007; Stark et al. 2007).

However, it is also possible to obtain constraints from the rest-frame UV-LFs. In contrast to the Ly $\alpha$  LF, the UV-LF is not affected by attenuation by the IGM, which allows for more reliable constraints on quantities related to the star formation efficiency. In the first part of this paper (§ 3–§ 4) we present limited modeling to illustrate parameter dependences, using the UV-LF to constrain model parameters related to star formation efficiency and lifetime. These model parameters may then be kept fixed, and the Ly $\alpha$  LFs and EW distributions used to constrain properties of high redshift LAEs such as their intrinsic Ly $\alpha$  EW and the fraction of Ly $\alpha$  that is transmitted through the IGM. Later, in § 5, we present our most general model, and fit to both the UV and Ly $\alpha$  LFs, as well as the EW distribution, simultaneously, treating all model parameters as free.

## 3 MODELING THE UV AND LY $\alpha$ LUMINOSITY FUNCTIONS.

### 3.1 Constraints from the UV-LF.

We begin by presenting a simple model for the UV-LF (Wyithe & Loeb 2007; Stark et al. 2007). In Figure 1 we show the rest-frame UV-LFs of LAEs at  $z = 5.7$  and  $z = 6.5$  (Shimasaku et al. 2006; Kashikawa et al. 2006). We use the following simple prescription to relate the ultraviolet flux density emitted by a galaxy,  $f_{1350}$ , to the mass of its host dark matter  $M_{\text{tot}}$ . The total mass of baryons within a galaxy is  $(\Omega_b/\Omega_m)M_{\text{tot}}$ , of which a fraction  $f_*$  is assumed to be converted into stars over a time scale of  $t_{\text{sys}} = \epsilon_{\text{DC}}t_{\text{hub}}$ . Here,  $\epsilon_{\text{DC}}$  is the duty cycle and  $t_{\text{hub}}(z)$ , the Hubble time at redshift  $z$ . This prescription yields a star formation rate of  $\dot{M}_* = f_*(\Omega_b/\Omega_m)M/t_{\text{sys}}$ . The star formation rate can then be converted into  $f_{1350}$  using the relation  $f_{1350} = 7 \times 10^{27}(\dot{M}_*/[M_\odot/\text{yr}]) \text{ erg s}^{-1} \text{ Hz}^{-1}$  (Kennicutt 1998). The precise relation is uncertain but differs by a factor of less than 2 between a normal and a metal-free stellar population (see e.g. Loeb et al. 2005). Uncertainty in this conversion factor does not affect our main conclusions. The presence of dust would lower the ratio of  $f_{1350}$  and  $\dot{M}_*$ , which could be compensated for by increasing  $f_*$ . However, Bouwens et al. (2006) found that dust in  $z = 6.0$  Lyman Break Galaxies (LBGs) attenuates the UV-flux by an average factor of only 1.4 (and dust obscuration may be even less important in LAEs, see § 6.3). Since this is within the uncertainty of the constraint we obtain on  $f_*$ , we ignore extinction by dust. The number density of LAEs with UV-flux densities exceeding  $f_{1350}$  is then given by

$$N(> f_{1350}) = \epsilon_{\text{DC}} \int_{M_{\text{UV}}}^{\infty} dM \frac{dn}{dM}, \quad (1)$$

where  $M_{\text{UV}}$  is the mass that corresponds to the flux density,  $f_{1350}$  (through the relations given above). The function  $dn/dM$  is the Press-Schechter (1974) mass function (with the modification of Sheth et al. 2001), which gives the number density of halos of mass  $M$  (in units of comoving  $\text{Mpc}^{-3}$ )<sup>1</sup>. The free parameters in our model are the duty cycle,  $\epsilon_{\text{DC}}$ , of the galaxy, and the fraction of baryons that are converted into stars,  $f_*$ . We calculated the UV-LF for a grid of models in the  $(\epsilon_{\text{DC}}, f_*)$ -plane, and generated likelihoods  $\mathcal{L}[P] = \exp[-0.5\chi^2]$ , where  $\chi^2 = \sum_i^{N_{\text{data}}} (\text{model}_i - \text{data}_i)^2/\sigma_i^2$ , in which  $\text{data}_i$  and  $\sigma_i$  are the  $i^{\text{th}}$  UV-LF data point and its error, and  $\text{model}_i$  is the model evaluated at the  $i^{\text{th}}$  luminosity bin. The sum is over  $N_{\text{data}} = 8$  data points. The inset in Figure 1 shows the resulting likelihood contours

<sup>1</sup> Our model effectively states that the star formation rate in a galaxy increases linearly with halo mass. This is probably not correct. To account for a different mass dependence we could write the star formation rate as  $\dot{M}_* \propto M^\beta$ , where  $\beta$  is left as a free parameter. However, the range of observed luminosities span only 1 order of magnitude, and we will show that the choice  $\beta = 1$  provides a model that describes the observations well. Furthermore, the duty cycle  $\epsilon_{\text{DC}}$  may be viewed as the fraction of dark matter halos that are currently forming stars. The remaining fraction  $(1 - \epsilon_{\text{DC}})$  of halos either have not formed stars yet, or are evolving passively. In either case, the contribution of these halos to the UV-LF is set to be negligible.

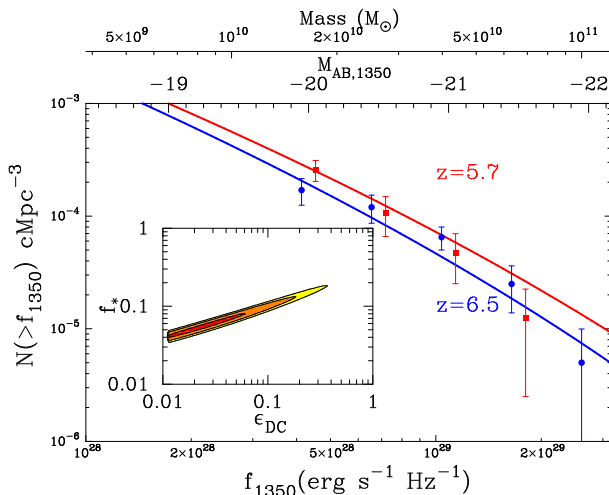


**Figure 1.** Constraints on the star formation efficiency from the observed rest-frame UV-luminosity functions of LAEs at  $z = 5.7$  (red squares) and  $z = 6.5$  (blue circles) (Shimasaku et al. 2006; Kashikawa et al. 2006). In our best-fit model, a fraction  $f_* \sim 0.06$  of all baryons is converted into stars over a time-scale of  $\epsilon_{\text{DC}} t_{\text{hub}} \sim 0.03$  Gyr (see text). The inset shows likelihood contours in the  $(\epsilon_{\text{DC}}, f_*)$ -plane at 64%, 26% and 10% of the peak likelihood. Also shown on the upper horizontal axis is the mass corresponding to  $M_{\text{AB},1350}$  in the best-fit model.

in the  $(\epsilon_{\text{DC}}, f_*)$ -plane at 64%, 26% and 10% of the peak likelihood. The best fit model has  $(\epsilon_{\text{DC}}, f_*) = (0.03, 0.06)$  and is plotted as the solid line. In the following sections we assume this combination of  $f_*$  and  $\epsilon_{\text{DC}}$ .

### 3.2 Constraints from the Ly $\alpha$ LF.

We next model the Ly $\alpha$  LF, beginning with the best-fit model of the previous section. The number density of LAEs at redshift  $z$  with Ly $\alpha$  luminosities exceeding  $\mathcal{T}_\alpha \times L_\alpha$  is given by (Dijkstra et al. 2007b)

$$N(> \mathcal{T}_\alpha \times L_\alpha, z) = \epsilon_{\text{DC}} \int_{M_\alpha}^{\infty} dM \frac{dn}{dM}(z), \quad (2)$$

where the Ly $\alpha$  luminosity and host halo mass,  $M_\alpha$  are related by

$$\mathcal{T}_\alpha \times L_\alpha = \mathcal{L}_\alpha \frac{M_\alpha (M_\odot) \frac{\Omega_b}{\Omega_m} f_*}{t_{\text{sys}}(\text{yr})} \mathcal{T}_\alpha. \quad (3)$$

In this relation,  $\mathcal{T}_\alpha$  is the IGM transmission multiplied by the escape fraction of Ly $\alpha$  photons from the galaxy, and  $\mathcal{L}_\alpha = 2.0 \times 10^{42} \text{ erg s}^{-1} / (M_\odot \text{ yr}^{-1})$ , is the Ly $\alpha$  luminosity emitted per unit of star formation rate (in  $M_\odot \text{ yr}^{-1}$ ). Throughout,  $\mathcal{L}_{\alpha,42}$  denotes  $\mathcal{L}_\alpha$  in units of  $10^{42} \text{ erg s}^{-1} / (M_\odot \text{ yr}^{-1})$ . We have taken  $\mathcal{L}_{\alpha,42} = 2.0$ , which is appropriate for a metallicity of  $Z = 0.05 Z_\odot$  and a Salpeter IMF (Dijkstra et al. 2007). Note that when comparing to observed luminosities (Shimasaku et al. 2006; Kashikawa et al. 2006), we have replaced  $L_\alpha$  with  $\mathcal{T}_\alpha \times L_\alpha$ . This is because the observed luminosities have been derived from the observed fluxes by assuming that all Ly $\alpha$  emerging from the galaxy was transmitted by the IGM, whereas there is substantial absorption (e.g. Dijkstra et al. 2007). The product  $\mathcal{T}_\alpha \times L_\alpha$  may be written as  $\mathcal{T}_\alpha \times L_\alpha = 4\pi d_L^2(z) S_\alpha$ , where  $S_\alpha$  is the total Ly $\alpha$  flux

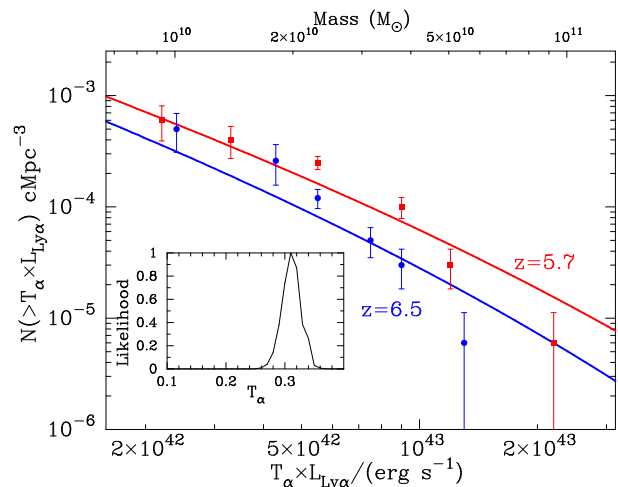


**Figure 2.** Joint constraints on the IGM transmission from the observed Ly $\alpha$  and rest-frame UV LFs of LAEs at  $z = 5.7$  (Shimasaku et al. 2006) and  $z = 6.5$  (Kashikawa et al. 2006). The red squares and blue circles represent the data at  $z = 5.7$  and  $z = 6.5$ . Using the model that best describes the UV-LFs with  $(f_{\text{star}}, \epsilon_{\text{DC}}) = (0.06, 0.03)$  we fit to the observed Ly $\alpha$  LF. The only free parameter of our model was the fraction of Ly $\alpha$  that was transmitted through the IGM at  $z = 5.7$ ,  $\mathcal{T}_{\alpha,57}$  (see text). Shown in the inset is the likelihood for  $\mathcal{T}_{\alpha,57}$ , normalised to a peak of unity. The figure shows that in order to simultaneously fit the Ly $\alpha$  and UV-LFs, only  $\sim 30\%$  of Ly $\alpha$  photons are transmitted through the IGM. The best fit models are overplotted as the solid lines.

detected on earth and  $d_L(z)$  is the luminosity distance to redshift  $z$ . The product  $\mathcal{T}_\alpha \times L_\alpha$  may therefore be viewed as an effective luminosity inferred at earth. Furthermore, the selection criteria used by Shimasaku et al. (2006) and Kashikawa et al. (2006) limits these surveys to be sensitive to LAEs with  $\text{EW} \gtrsim 10 \text{ \AA}$ . In the remainder of this paper, the EW of model LAEs is always larger than this  $\text{EW}_{\text{min}}$ , and we need not worry about selection effects when comparing our model to the data.

In this section, we set the transmission at  $z = 6.5$  (denoted by  $\mathcal{T}_{\alpha,65}$ ) to be a factor of  $\sim 1.2$  lower<sup>2</sup> than at  $z = 5.7$  (denoted by  $\mathcal{T}_{\alpha,57}$ ). This ratio is the median of the range found by Dijkstra et al. (2007). We then calculated the Ly $\alpha$  LF for a range of  $\mathcal{T}_{\alpha,57}$ , and generated likelihoods  $\mathcal{L}[P] = \exp[-0.5\chi^2]$ , where  $\chi^2 = \sum_i^{N_{\text{data}}} (\text{model}_i - \text{data}_i)^2 / \sigma_i^2$ , for each model. Here,  $\text{data}_i$  and  $\sigma_i$  are the  $i^{\text{th}}$  data point and its error, and  $\text{model}_i$  is the model evaluated at the  $i^{\text{th}}$  luminosity bin. The sum is over  $N_{\text{data}} = 6$  points at each redshift. In Figure 2 we show the Ly $\alpha$  luminosity functions at  $z = 5.7$  and  $z = 6.5$ . The red squares and blue circles represent data from Shimasaku et al. (2006,  $z = 5.7$ ) and Kashikawa et al. (2006,  $z = 6.5$ ), respectively.

The likelihood for  $\mathcal{T}_{\alpha,57}$  (normalised to a peak of unity) is shown in the inset. The best fit model is overplotted as the solid lines, for which the value of the transmission is  $\mathcal{T}_{\alpha,57} = 0.30$ . The modeling presented in this and the

<sup>2</sup> For our primary results in § 5 we allow this ratio to be a free parameter. The results presented in this section is not sensitive to the precise choice of the ratio of IGM transmission at  $z = 5.7$  and  $z = 6.5$ .

previous section therefore suggests that, in order to simultaneously fit the Ly $\alpha$  and UV luminosity functions, only  $\sim 30\%$  of the Ly $\alpha$  can be transmitted through the IGM. This transmission is in good agreement with the results obtained by Dijkstra et al. (2007), who modeled the transmission directly and found that for reasonable model parameters the transmission must lie in the range  $0.1 \lesssim \mathcal{T}_\alpha \lesssim 0.3$ .

### 3.3 The Predicted Equivalent Width

While in agreement with the observed LFs, the model described in § 3.2 does not reproduce the very large observed equivalent widths. The Ly $\alpha$  luminosity can be rewritten in terms of the star formation rate ( $\dot{M}_*$ ) and EW as  $L_\alpha = 2.0 \times 10^{42} \text{ erg s}^{-1} \dot{M}_* (M_\odot/\text{yr})(\text{EW}/160 \text{ \AA})$ . Here we have used the relation  $L_\alpha = \text{EW} \times [\nu_\alpha f(\nu_\alpha)/\lambda_\alpha]$ , where  $f(\nu_\alpha)$  is the flux density in  $\text{erg s}^{-1} \text{ Hz}^{-1}$  at  $\nu_\alpha$ , and where we denoted the Ly $\alpha$  frequency and wavelength by  $\nu_\alpha$  and  $\lambda_\alpha$  respectively. Furthermore, we assumed the spectrum to be constant between 1216  $\text{\AA}$  and 1350  $\text{\AA}$ . For  $\mathcal{L}_{\alpha,42} = 2.0$ , we find a best fit model that predicts LAEs to have an observed EW of  $\mathcal{T}_\alpha \times 160 \text{ \AA} \sim 50 \text{ \AA}$ . This value compares unfavorably with the observed sample that includes EWs exceeding  $\sim 100 \text{ \AA}$  in  $\sim 50\%$  of cases for Ly $\alpha$  selected galaxies (Shimasaku et al. 2006).

Thus although our simple model can successfully reproduce the observed Ly $\alpha$  and UV luminosity functions, the model fails to reproduce the observed large EW LAEs. This discrepancy cannot be remedied by changing the intrinsic Ly $\alpha$  emissivity of a given galaxy,  $\mathcal{L}_\alpha$ : increasing  $\mathcal{L}_\alpha$  would be simply be compensated for by a lower  $\mathcal{T}_\alpha$  and vice versa. In the next section we discuss a simple modification of this model that aims to alleviate this discrepancy.

## 4 THE FLUCTUATING IGM MODEL

The model described in § 3 assumed that the Ly $\alpha$  flux of galaxies was subject to uniform attenuation by the IGM. In this section we relax this assumption and investigate the predicted EWs in a more realistic IGM where transmission fluctuates between galaxies. We refer to this model as the ‘fluctuating IGM’ model. In this model, a larger transmission translates to a larger observed equivalent width. As a result, galaxies with large  $\mathcal{T}_\alpha$  are more easily detected, and the existence of these galaxies may therefore affect the observed EW-distribution for Ly $\alpha$  selected galaxies, even in cases where they comprise only a small fraction of the intrinsic population. In this section we investigate whether this bias could explain the anomalously large observed EW.

We assume a log-normal distribution for  $\mathcal{T}_{\alpha,57}$ ,

$$P(u)du = \frac{1}{\sqrt{2\pi}\sigma_u} \times \exp\left(-\frac{(u - \langle u \rangle)^2}{2\sigma_u^2}\right) du, \quad (4)$$

where  $\langle u \rangle = \log(\mathcal{T}_{\alpha,57})$  is the log (base 10) of the mean transmission and  $\sigma_u$  is the standard deviation in log-space. Throughout this section we drop the subscript ‘57’. Eq (4) may be rewritten in the form

$$f(> u) = \frac{1}{2} - \frac{1}{2} \text{erf}\left(\frac{u - \langle u \rangle}{\sqrt{2}\sigma_u}\right), \quad (5)$$

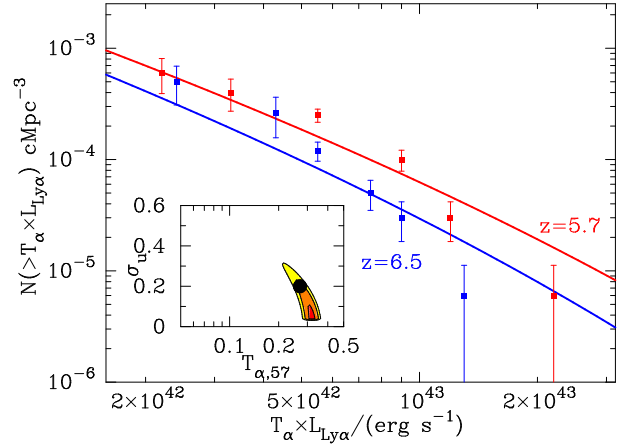


**Figure 3.** Same as Figure 2. However, instead of assuming a single value of IGM transmission  $\mathcal{T}_{\alpha,57}$ , we assumed a log-normal distribution of IGM transmission with a mean of  $\log \mathcal{T}_{\alpha,57}$  and standard deviation of (in the log)  $\sigma_u$  (see text). This reflects the possibility that the IGM transmission fluctuates between galaxies. The inset shows likelihood contours for  $(\log \mathcal{T}_{\alpha,57}, \sigma_u)$ . Increasing  $\sigma_u$  flattens the luminosity function (and moves it upward), which is illustrated by the model LFs shown as *solid lines*, for which we used  $(\mathcal{T}_{\alpha,57}, \sigma_u) = (0.27, 0.2)$  (shown as the *thick black dot* in the inset). The best-fit model to the data has  $\sigma_u \sim 0$  (which corresponds to the model shown in Figure 2).

which gives the fraction of LAEs with  $\log \mathcal{T}_\alpha > u$ . The number density of LAEs is then given by

$$N(> \mathcal{T}_\alpha \times L_\alpha) = \epsilon_{\text{DC}} \int_0^\infty dM \frac{dn}{dM} f(> u(\mathcal{T}_\alpha \times L_\alpha, M)) \quad (6)$$

where

$$u(\mathcal{T}_\alpha \times L_\alpha, M) = \log\left(\frac{\mathcal{T}_\alpha \times L_\alpha}{\mathcal{L}_\alpha \dot{M}_*}\right). \quad (7)$$

Eq (6) differs from Eq (2) in two ways: (1) there is no lower integration limit, and (2) there is an additional term  $f(> u)$ . These two differences reflect the facts that all masses contribute to the number density of LAEs brighter than  $\mathcal{T}_\alpha \times L_\alpha$ , and that lower mass systems require larger transmissions (Eq 7) which are less common (Eq 5). In the limit  $\sigma_u \rightarrow 0$ , the function  $f(> u)$  ‘jumps’ from 0 to 1 at  $M_{\text{min}}$  (Eq 3), which corresponds to the original Eq (2).

In this formalism we may also write the number density of LAEs with transmission in the range  $u \pm du/2 \equiv \log \mathcal{T}_\alpha \pm \frac{d \log \mathcal{T}_\alpha}{2}$ , which is given by

$$N(u)du = P(u)du \int_{M_{\text{min}}(u)}^\infty dM \frac{dn}{dM}. \quad (8)$$

Here  $M_{\text{min}}(u)$  is the minimum mass of galaxies that can be detected with a transmission in the range  $u \pm du/2$  (for  $M_{\text{tot}} < M_{\text{min}}$  the total flux falls below the detection threshold). The number density of LAEs with transmission in the range  $u \pm du/2$  may be used to find the number density of LAEs with equivalent widths in the range  $\log \text{EW} \pm \frac{d \log \text{EW}}{2}$  via the relation  $\text{EW} = 160 \mathcal{T}_\alpha \text{ \AA}$  (for the choice  $\mathcal{L}_{\alpha,42} = 2.0$ , see § 3.2). Eq (8) shows that the observed equivalent width distribution takes the shape of the original transmission distribution, modulo a boost which increases towards larger EWs.

As in § 3.2 we assume the best-fit model parameters

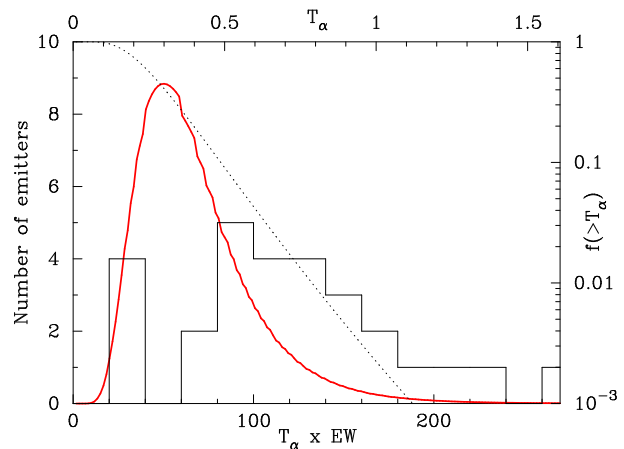
for  $\epsilon_{\text{DC}}$  and  $f_*$  derived from the UV-LFs determined in § 3.1. We calculate model Ly $\alpha$  LFs on a grid of models in the  $(\sigma_u, \langle \mathcal{T}_\alpha \rangle)$ -plane, and generate likelihoods following the procedure outlined in § 3.2. The results of this calculation are shown in Figure 3 where we plot the Ly $\alpha$  LFs together with likelihood contours in the  $(\sigma_u, \langle \mathcal{T}_\alpha \rangle)$ -plane (inset). The best-fit models favor no scatter in  $\mathcal{T}_\alpha$  ( $\sigma_u \sim 0$ ). The reason for this is that for any given model, a scatter in  $\mathcal{T}_\alpha$  serves to flatten the model LF. However, the observed Ly $\alpha$  LF is quite steep, and as a result the data prefers a model with no scatter. Furthermore, a scatter in  $\mathcal{T}_\alpha$  results in a model LF that lies above the original (constant transmission) LF at all  $\mathcal{T}_\alpha \times L_\alpha$ . This also explains the shape of the contours in the  $(\sigma_u, \langle \mathcal{T}_\alpha \rangle)$ -plane; increasing  $\sigma_u$  must be compensated for by lowering  $\langle \mathcal{T}_\alpha \rangle$ . To illustrate the impact of a fluctuating  $\mathcal{T}_\alpha$ , the model LFs shown in Figure 3 are not those of the best-fit model, but of a model with  $(\langle \mathcal{T}_\alpha \rangle, \sigma_u) = (0.27, 0.2)$ .

Figure 4 shows the observed EW-distribution (*solid line*) at  $z = 5.7$  associated with the Ly $\alpha$  LFs shown in Figure 3. This model may be compared to the observed distribution (shown as the *histogram*, data from Shimasaku et al, 2006). The upper horizontal axis shows the transmission corresponding to each equivalent width. The *dotted line* shows the distribution of transmission (given by Eq 4). Note that the range of transmissions shown in Figure 4 extends to  $\mathcal{T}_\alpha > 1$ , which of course is not physical. The model EW-distribution has a tail towards larger EWs. However, the model distribution peaks at  $\text{EW} \sim 50 \text{ \AA}$ . As was seen in the constant transmission model, this is clearly inconsistent with the observations, which favor values of  $\text{EW} \sim 100 \text{ \AA}$ . Shimasaku et al. (2006) also show a probability distribution of EW, which is probably closer to the actual distribution. Although this distribution does peak closer to  $\text{EW} \sim 50 \text{ \AA}$ , it is still significantly broader than that of the model (see § 6 for more arguments against the fluctuating IGM model). We point out that the model distribution shown in Figure 4 is independent of the assumed value of  $\mathcal{L}_{\alpha,42}$ .

## 5 LY $\alpha$ EMITTERS POWERED BY VERY MASSIVE STARS.

In § 3 we demonstrated that a simple model where  $L_\alpha$  and  $L_{\text{UV}}$  were linearly related to halo mass can reproduce the UV and Ly $\alpha$  LFs, but not the observed EW distribution. In § 4 we showed that this situation is not remedied by a variable IGM transmission, and that favored models have a constant transmission. In this section we discuss an alternate model, which leads to consistency with both the observed Ly $\alpha$  LFs, UV-LFs, and the EW-distribution. In this model, galaxies are assumed to have a bright Ly $\alpha$  phase (hereafter the ‘population III’-phase) which lasts a fraction  $f_{\text{III}}$  of the galaxies’ life-time. After this the galaxy’s Ly $\alpha$  luminosity drops to the ‘normal’ value for population II star formation.

This model may be viewed as an extension of the idea originally described by Malhotra & Rhoads (2002), that large EW LAEs are young galaxies in the early stages of their lives. In this picture, the sudden drop in Ly $\alpha$  luminosity could represent i) a sudden drop in the ionising luminosity when the first O-stars died, or ii) an enhanced dust-opacity after enrichment by the first type-II supernovae. Alternatively, our parametrisation could represent a scenario



**Figure 4.** Comparison of the observed equivalent width distribution (EW, *histogram*), with the model prediction for a model in which we assumed a log-normal distribution of IGM transmission with  $(\mathcal{T}_{\alpha,57}, \sigma_u) = (0.27, 0.2)$  (see Fig 3). The EW is related to  $\mathcal{T}_\alpha$  via  $\text{EW} = 160 \mathcal{T}_\alpha \text{ \AA}$ . The *dotted line* shows the fraction,  $f(> \mathcal{T}_\alpha)$  (shown on the right vertical axis), of galaxies with a transmission greater than  $\mathcal{T}_\alpha$  (Eq 5). Galaxies with large  $\mathcal{T}_\alpha$  are more easily detected, hence the large  $\mathcal{T}_\alpha$  (EW) end is boosted considerably, resulting in closer agreement (but not close enough) to the data.

in which the population III phase ended after the first population III stars enriched the surrounding interstellar gas from which subsequent generations of stars formed. Hence, we refer to this model as the ‘population III’ model. We will show that to be consistent with the large values of the observed EW, a very massive population of stars is required during the early stages of star formation.

To minimise the number of free parameters we modeled the time dependence of the Ly $\alpha$  EW as a step-function. The number density of LAEs is then given by

$$N(> \mathcal{T}_\alpha \times L_\alpha, z) = f_{\text{III}} \times \epsilon_{\text{DC}} \int_{M_{\alpha, \text{III}}}^{\infty} dM \frac{dn}{dM}(z) + (1 - f_{\text{III}}) \times \epsilon_{\text{DC}} \int_{M_{\alpha, \text{II}}}^{\infty} dM \frac{dn}{dM}(z). \quad (9)$$

Here,  $M_{\alpha, \text{II}}$  is the mass related to  $\mathcal{T}_\alpha \times L_\alpha$  through  $\mathcal{T}_\alpha \times L_\alpha = \mathcal{L}_\alpha \times \mathcal{T}_\alpha \times M_*$ , while  $M_{\alpha, \text{III}}$  is the population III mass, which is calculated with  $\mathcal{L}_\alpha$  replaced by  $\mathcal{L}_\alpha = (\text{EW}_{\text{III}}/160 \text{ \AA}) \times 2 \times 10^{42} \text{ erg s}^{-1}$ .

Whereas in previous sections we chose fiducial or best fit parameters for illustration, for the model described in this section we take the most general approach. We fit the model simultaneously to the UV-LF and Ly $\alpha$  LFs, as well as to the observed EW-distribution of Ly $\alpha$  selected galaxies. This model predicts two observed equivalent widths ( $\mathcal{T}_\alpha \times \text{EW}_{\text{III}}$  and  $\mathcal{T}_\alpha \times \text{EW}_{\text{II}}$ ) in various abundances. The associated mean and variance from the model are compared to the observed EW-distribution, which has a mean of  $\langle \text{EW} \rangle = 120 \pm 25 \text{ \AA}$ , and a standard deviation of  $\sigma_{\text{EW}} = 50 \pm 10 \text{ \AA}$ .

Our model has 6 free parameters ( $\epsilon_{\text{DC}}, f_*, \mathcal{T}_{\alpha,57}, \mathcal{T}_{\alpha,65}, f_{\text{III}}, \text{EW}_{\text{III}}$ ). We produce likelihoods for each parameter by marginalising over the others in this space. The lower set of panels in Figure 5 show likelihood contours for our model parameters at 64%, 26% and 10% of the peak likelihood. The best-fit models have  $\text{EW}_{\text{III}} \sim 600 - 800 \text{ \AA}$  and  $f_{\text{III}} = 0.04 - 0.1$  which

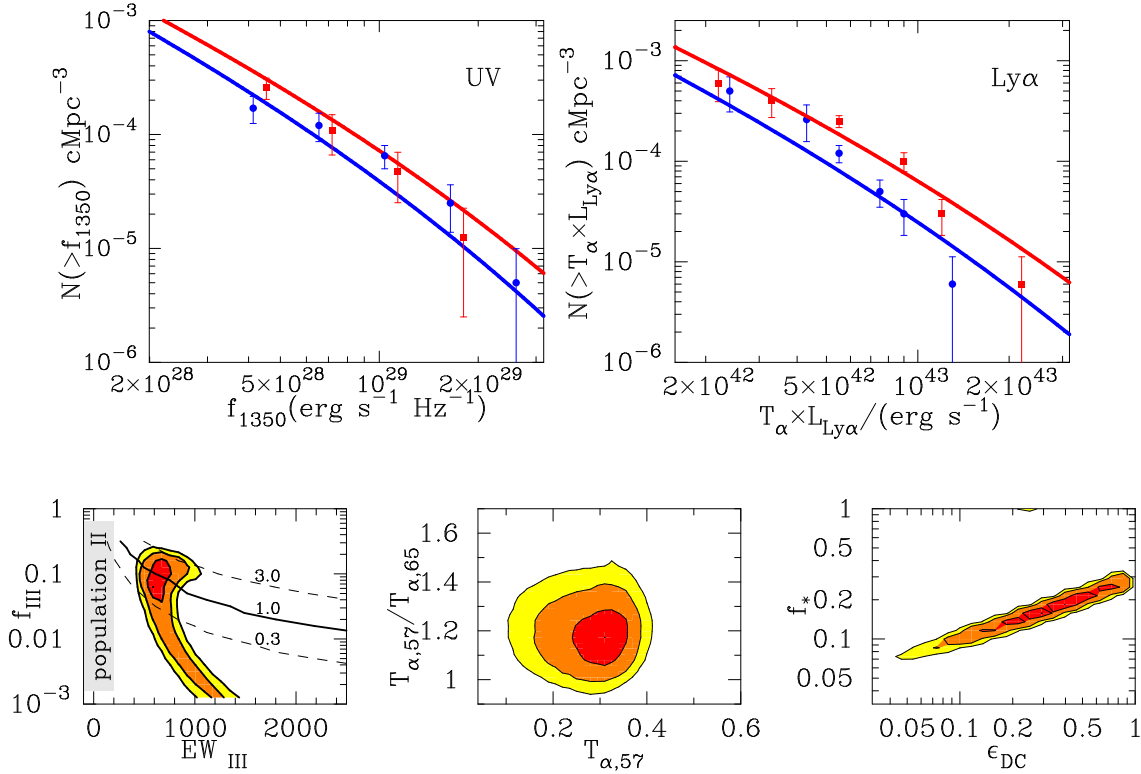


**Figure 5.** Marginalised constraints on the 6 population-III model parameters,  $(\epsilon_{\text{DC}}, f_*, \mathcal{T}_{\alpha,57}, \mathcal{T}_{\alpha,65}, f_{\text{III}}, \text{EW}_{\text{III}})$ , are shown in the lower three panels. In the best-fit population-III model, each galaxy goes through a luminous Ly $\alpha$  phase during which the equivalent width is  $\text{EW}_{\text{III}} = 600 - 800 \text{ \AA}$  for a fraction  $f_{\text{III}} = 0.04 - 0.1$  of the galaxies life time. Although the bright phase only lasts a few to ten per cent of their life-time, galaxies in the bright phase are more easily detectable, and the number of galaxies detected in Ly $\alpha$  surveys in the bright phase is equal to that detected in the faint phase. This is also demonstrated by the *thick solid line* (with label '1.0') in the *lower left panel*, which shows the combination of  $f_{\text{III}}$  and  $\text{EW}_{\text{III}}$  that produces equal numbers of galaxies in the population III and II phase (the *dashed lines* are defined similarly, also see Fig 6). The best-fit intrinsic equivalent widths are in excess of the maximum allowed for a population-II stellar population having a Salpeter mass function. Therefore, this model requires a burst of very massive star formation lasting no more than a few to ten per cent of the galaxies star forming lifetime, and may indicate the presence of population-III star formation in a large number of high-redshift LAEs.

corresponds to a physical timescale for the population-III phase of  $f_{\text{III}} \times \epsilon_{\text{DC}} \times t_{\text{hub}} \sim 4 - 50 \text{ Myr}$  (for  $0.1 \lesssim \epsilon_{\text{DC}} \lesssim 0.5$ ). The model Ly $\alpha$  luminosity functions at  $z=5.7$  and  $z=6.5$  described by  $(\epsilon_{\text{DC}}, f_*, \mathcal{T}_{\alpha,57}, \mathcal{T}_{\alpha,65}, f_{\text{III}}, \text{EW}_{\text{III}}) = (0.2, 0.14, 0.22, 0.19, 0.08, 650 \text{ \AA})$  are shown as solid lines and provide good fits to the data. The model produces two observed EWs, namely  $\mathcal{T}_{\alpha} \times \text{EW}_{\text{II}} = 35 \text{ \AA}$  and  $\mathcal{T}_{\alpha} \times \text{EW}_{\text{III}} = 143 \text{ \AA}$ . It is worth emphasising that the emitted EW of the bright phase depends on the choice  $\mathcal{L}_{\alpha,42}$  via  $\text{EW}_{\text{III}} = 650(\mathcal{L}_{\alpha,42}/2.0) \text{ \AA}$ . Hence, a lower/higher value of  $\mathcal{L}_{\alpha,42}$  would decrease/increase the intrinsic brightness of the 'population III' phase. Note that  $\mathcal{L}_{\alpha,42} = 1.0$  when LAEs formed out of gas of solar metallicity, which is unreasonable given the universe was only  $\sim 1 \text{ Gyr}$  old at  $z = 6$ . Furthermore,  $\mathcal{L}_{\alpha,42} = 1$  would have yielded a best-fit  $\mathcal{T}_{\alpha,57} = 0.5$ , which is well outside the range calculated by Dijkstra et al. (2007). We there conclude that  $\mathcal{L}_{\alpha,42}$  is in excess of unity.

In performing fits we have fixed the value of  $\text{EW}_{\text{II}}$  to correspond to a standard stellar population, and then explored the possibility that there might be a second phase of SF producing a larger EW. Our modeling finds strong statistical evidence for this early phase and rules out the null-hypothesis that properties can be described by population-II

stars alone at high confidence (*grey region* in the *lower left panel* inset of Fig 5). Despite the fact that the best fit model has a bright phase which lasts only a few per cent of the total star formation lifetime, the two populations of LAEs are similarly abundant in model realisations of the observed sample in Ly $\alpha$  selected galaxies (see § 5.1 for a more detailed comparison to the observed EW distributions). This is shown in the *lower left panel* in Figure 5 in which the *solid line* (with label '1.0') shows the combination of  $f_{\text{III}}$  and  $\text{EW}_{\text{III}}$  for which the observed number of galaxies in the population III phase ( $N_{\text{III}}$ ) equals that in the population II phase ( $N_{\text{II}}$ ). The *dashed lines* show the cases  $N_{\text{III}}/N_{\text{II}} = 0.3$  and  $N_{\text{III}}/N_{\text{II}} = 3.0$ . The duration of the bright Ly $\alpha$  phase meets theoretical expectations for a burst of star formation, while the large EW requires a very massive stellar population (e.g Schaefer 2003; Tumlinson et al. 2003). In summary, in order to reproduce both the UV and Ly $\alpha$  LFs, and the observed population of large EW galaxies, we require a burst of very massive star formation lasting  $\lesssim 10$  per cent of the galaxies lifetime.

### 5.1 EW Distribution of UV and Ly $\alpha$ Selected Galaxies

Stanway et al. (2007) show that 11 out of 14 LAE candidates among i-drop galaxies in the Hubble Ultra Deep Field have  $EW < 100 \text{ \AA}$ . If galaxies are included for which only upper or lower limits on the EW are available, then this fraction becomes 21 out of 26. Thus the distribution of EWs for i-drop selected galaxies differs strongly from the EW-distribution observed by Shimasaku et al. (2006). We next describe why this strong dependence of the observed Ly $\alpha$  EW distribution on the precise galaxy selection criteria arises naturally in our population III model.

We first assume that the Ly $\alpha$  selected and UV-selected galaxies were drawn from the same population (this assumption is discussed further in § 6.3). In our model a galaxy that is selected based on its rest-frame UV-continuum emission has a probability  $f_{\text{III}}$  of being observed in the Ly $\alpha$  bright phase, while the probability of finding a galaxies in the Ly $\alpha$  faint phase is  $1 - f_{\text{III}}$ . In § 5 we found  $f_{\text{III}} \sim 0.1$ , hence an i-drop galaxy is  $\sim 10$  times more likely to have a low than a high observed EW. If we denote the number of galaxies with  $EW > 100 \text{ \AA}$  by  $N_{\text{III}}$ , and the number of galaxies with  $EW < 100 \text{ \AA}$  by  $N_{\text{II}}$ , then the model predicts  $N_{\text{III}}/N_{\text{II}} = f_{\text{III}}/(1 - f_{\text{III}}) \sim 0.1$ , while the observed fraction including the galaxies for which the EW is known as upper or lower limit is  $N_{\text{III}}/N_{\text{II}} = 0.19 \pm 0.05$ . Therefore the qualitative difference in observed Ly $\alpha$  EW distribution among i-drop galaxies in the HUDF and among Ly $\alpha$  selected galaxies follows naturally from our two-phase star formation model. Note that our model predicts population III star formation to be observed in  $f_{\text{III}}/(1 - f_{\text{III}}) \sim 10\%$  of the  $z = 6.0$  LBG population.

The dependence of the observed EW distribution on the selection criteria used to construct the sample of galaxies is illustrated in Figure 6. To construct this figure, we have taken the best-fit population III model of § 5. For the purpose of presentation, we let the IGM fluctuate according to the prescription of § 4 with  $\sigma_u = 0.1$ , so that the model predicts a finite range of EWs in each phase. The *left and right panels* show the predicted EW distribution for Ly $\alpha$  selected (*left panel*) and UV-selected (*right panel*) galaxies as the *solid lines*, respectively. For a UV-selected galaxy the probability of being in the bright phase and having an observed EW in the range  $EW_{\text{III}} \times (\mathcal{T}_\alpha \pm d\mathcal{T}_\alpha/2)$  is  $f_{\text{III}}P(\mathcal{T}_\alpha)d\mathcal{T}_\alpha$ . Here  $P(\mathcal{T}_\alpha)d\mathcal{T}_\alpha$  is the probability that the IGM transmission is in the range  $\mathcal{T}_\alpha \pm d\mathcal{T}_\alpha/2$ , which is derived from Eq 4. The units on the vertical axis are arbitrary, and chosen to illustrate the different predicted and observed Ly $\alpha$  EW distributions for the two samples at large EWs. The observed distributions for Ly $\alpha$  and UV selected galaxies, shown as *histograms*, are taken from Shimasaku et al. (2006) and Stanway et al. (2007), respectively. Figure 6 clearly shows that both the predicted and observed Ly $\alpha$  selected samples contain significantly more large EW LAEs than the UV-selected sample. Our model naturally explains the qualitative shape of these distributions and their differences.

Before proceeding we mention a caveat to the distributions shown in Figure 6. In our model all galaxies have an EW of  $\mathcal{T}_\alpha \times EW_{\text{II}} \sim 25\text{--}35 \text{ \AA}$  during the population II phase, while in contrast Stanway et al. (2007) do not detect 10 out of 26 LBGs, which implies that  $\sim 40\%$  of LBGs have an

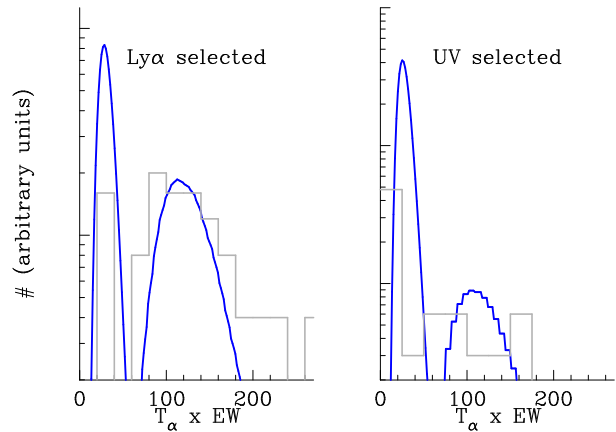


**Figure 6.** Comparison of the predicted EW distribution for UV and Ly $\alpha$  selected galaxies. The best-fit population-III model (see § 5) was used. In order to get a finite range of observed EWs (instead of only two values at  $\mathcal{T}_\alpha \times EW_{\text{II}}$  and  $\mathcal{T}_\alpha \times EW_{\text{III}}$ , we assumed the IGM transmission to fluctuate. The units on the vertical axis are arbitrary. The figure shows that in our population III model, the Ly $\alpha$  selected sample contains a larger relative fraction of large EW LAEs than the UV-selected (i-drop) sample, which is qualitatively in good agreement with the observations (shown by the *histograms*).

$EW \lesssim 6 \text{ \AA}$ . Thus there is a discrepancy between our model and the observations with respect to the value of EW in the population II phase. The resolution of this discrepancy lies in the fact that the very low EW emitters are drawn from the UV (i-drop) sample and not the Ly $\alpha$  selected sample our model was set up to describe. This issue is discussed in more detail in § 6.3.

An EW distribution of dropout sources was also presented by Dow-Hygelund et al. (2007). These authors performed an analysis similar to Stanway et al. (2007) and found 1 LAE with  $EW = 150 \text{ \AA}$  among 22 candidate  $z=6.0$  LBGs. When interpreted in reference to our model, this translates to  $N_{\text{III}}/N_{\text{II}} \sim 5\%$ , which is consistent with the model predictions. Therefore, when interpreted in light of a two-phase star formation history and different selection methods, the EW distribution observed by Dow-Hygelund et al. (2007) is consistent with that found by Shimasaku et al. (2006).

If population III star formation does provide the explanation for the very large EW Ly $\alpha$  emitters, then we would expect the large EW emitters to become less common with time as the mean metallicity of the Universe increased. To test this idea, we can compare the EW-distribution at  $z = 5.7$  with the results at lower redshift from Shapley et al. (2003) who found that  $\lesssim 0.5\%$  of  $z = 3$  LBGs have Ly $\alpha$   $EW \geq 150 \text{ \AA}$ , and that  $\lesssim 2\%$  of  $z = 3$  LBGs to have Ly $\alpha$   $EW \geq 100 \text{ \AA}$ . Dow-Hygelund et al. (2007) argue that the fraction of large EW Ly $\alpha$  lines at  $z = 6$  is consistent with that observed at  $z = 3$  (Shapley et al. 2003). However, if the EW distribution did not evolve with redshift, then the probability that a sample of 22 LBGs will contain at least 1 LAE with  $EW \gtrsim 150 \text{ \AA}$  is  $\lesssim 10\%$ . Thus the hypothesis that the observed EW distribution remains constant is ruled out at the  $\sim 90\%$  level. On the other hand, in a similar analysis Stanway et al. (2007) found 5 out of 26 LBGs to have an  $EW \gtrsim 100 \text{ \AA}$ . If the EW distribution did not evolve

with redshift, then the probability of finding 5 EW  $\gtrsim 100$  Å in this sample is only  $\sim 10^{-4}$ . Furthermore, Nagao et al. (2007) recently found at least 5 LAEs with  $\text{EW} > 100$  Å at  $6.0 \lesssim z \lesssim 6.5$ , and conclude that 8% of i-drop galaxies in the Subaru Deep Field have  $\text{EW} > 100$  Å, which is significantly larger than the fraction of large EW LBGs at  $z = 3$ . Therefore, the observed EW distribution of LBGs at  $z = 6$  is skewed more toward large EWs than at  $z = 3$ . The strength of this result is increased by the fact that the IGM is more opaque to Ly $\alpha$  photons at  $z = 6$  than at  $z = 3$ . Thus we conclude that the intrinsic EW distribution must have evolved with redshift.

## 6 DISCUSSION

### 6.1 Comparison with Population Synthesis Models

Population synthesis models have suggested that the broad band colors of observed LAEs are best described with young stellar populations (Gawiser et al. 2006; Pirzkal et al. 2007; Finkelstein et al. 2007). Lai et al. (2007) found the stellar populations in three LAEs to be 5 – 100 Myr old, and possibly as old as 700 Myr (where the precise age upper limit depends on the assumed star formation history of the galaxies). However as was argued by Pirzkal et al. (2007), since these galaxies were selected based on their detection in IRAC, a selection bias towards older stellar populations may exist (also see Lai et al. 2007). Furthermore, Finkelstein et al. (2007) found that LAEs with  $\text{EW} > 110$  Å have ages  $\lesssim 4$  Myr, while LAEs with  $\text{EW} < 40$  Å have ages between 20–400 Myr. This latter result in particular agrees well with our population III model. On the other hand, in a fluctuating IGM model for example, the EW of LAEs should be uncorrelated with age.

In models presented in this paper, on average  $f_* \sim 0.15$  of all baryons are converted into stars within halos of mass  $M_{\text{tot}} \sim 10^{10} - 10^{11} M_{\odot}$ , yielding stellar masses in the range  $M_* = 10^8 - 10^9 M_{\odot}$  (Dijkstra et al. 2007b; Stark et al. 2007). This compares unfavorably with the typical stellar masses found observationally in LAEs which can be as low as  $M_* = 10^6 - 10^7 M_{\odot}$  (Finkelstein et al. 2007; Pirzkal et al. 2007). However, the lowest stellar masses are found (naturally) for the younger galaxies. Indeed, the LAEs with the oldest stellar populations can have stellar masses as large as  $10^{10} M_{\odot}$ . Thus, we do not find the derived stellar masses in LAEs to be at odds with the results of this paper. If significant very massive (or population III) star formation indeed occurred in high redshift LAEs, then one may expect these stars to reveal themselves in unusual broad-band colors (e.g. Stanway et al. 2005). However, Tumlinson et al. (2003) have shown that the most distinctive feature in the spectrum of population III stars is the number of H and He ionising photons (also see Bromm et al. 2001). Since these are (mostly) absorbed in the IGM, the broad band spectrum of population III stars is in practice difficult to distinguish from a normal stellar population (Tumlinson et al. 2003), especially when nebular continuum emission is taken into account (Schaerer & Pelló 2005, see their Fig 1). Hence, population III stars would not necessarily be accompanied by unusually blue broad band colors.

### 6.2 Alternative Explanations for Large EW LAEs

We have shown that a simple model in which high-redshift galaxies go through a population-III phase lasting  $\lesssim 15$  Myr can simultaneously explain the observed Ly $\alpha$  LFs at  $z = 5.7$  and  $z = 6.5$  (Kashikawa et al. 2006), and the observed EW-distribution of Ly $\alpha$  selected galaxies at  $z = 5.7$  (Shimasaku et al. 2006). In addition, this model predicts the much lower EWs found in the population of UV selected galaxies (Stanway et al. 2007, see § 5.1). Moreover the constraints on the population-III model parameters such as the duration and the equivalent width of the bright phase are physically plausible, and consistent with existing population synthesis work (see § 6.1).

Are there other interpretations of the large observed EWs? One possibility was discussed in § 4, where we showed that the simple model in which the IGM transmission fluctuates between galaxies reproduces the LFs, but fails to simultaneously reproduce the Ly $\alpha$  LFs and the observed EW-distribution. In addition, this model fails to reproduce other observations. Dijkstra et al. (2007) calculated the impact of the high-redshift reionised IGM on Ly $\alpha$  emission lines and found the range of plausible transmissions to lie in the range  $0.1 < \mathcal{T}_{\alpha} < 0.3$ . This work showed that it is possible to boost the transmission to (much) larger values but not without increasing the observed width of the Ly $\alpha$  line. Absorption in the IGM typically erases all flux blueward of the Ly $\alpha$  resonance, and when infall is accounted for, part of the Ly $\alpha$  redward of the Ly $\alpha$  resonance as well. This implies that Ly $\alpha$  lines that are affected by absorption in the IGM are systematically narrower than they would have been if no absorption in the IGM had taken place. It follows that in the fluctuating IGM model, Ly $\alpha$  EW should be strongly correlated with the observed Ly $\alpha$  line width (or FWHM). This correlation is not observed. In fact, observations suggest that an anti-correlation exists between EW and FWHM (Shimasaku et al. 2006; Tapken et al. 2007). This anti-correlation provides strong evidence against the anomalously large EWs being produced by a fluctuating IGM transmission.

A second possibility is the presence of galaxies with strong superwinds. The models of Dijkstra et al. (2007) did not study the impact of superwinds on the Ly $\alpha$  line profile. The presence of superwinds can cause the Ly $\alpha$  line to emerge with a systematic redshift relative to the Ly $\alpha$  resonance through back scattering of Ly $\alpha$  photons off the far side of the shell that surrounds the galaxy (Ahn et al. 2003; Ahn 2004; Hansen & Oh 2006; Verhamme et al. 2006). However, superwinds tend not only to redshift the Ly $\alpha$  line, they also make the Ly $\alpha$  line appear broader than when this scattering does not occur. As in the case of the fluctuating IGM model, this results in a predicted correlation between EW and FWHM, which is not observed. Furthermore in wind-models, the overall redshift of the Ly $\alpha$  line, and thus  $\mathcal{T}_{\alpha}$ , increases with wind velocity,  $v_w$ . This predicts that EW increases with wind velocity. However, observations of  $z = 3$  LBGs by Shapley et al. (2003) show that EW correlates with  $v_w^{-1}$  (Ferrara & Ricotti 2006). We therefore conclude that the large EW in LAEs cannot be produced by superwind galaxies.

A third possibility might be that within the Ly $\alpha$  emitting galaxy, cold, dusty clouds lie embedded in a hot inter-

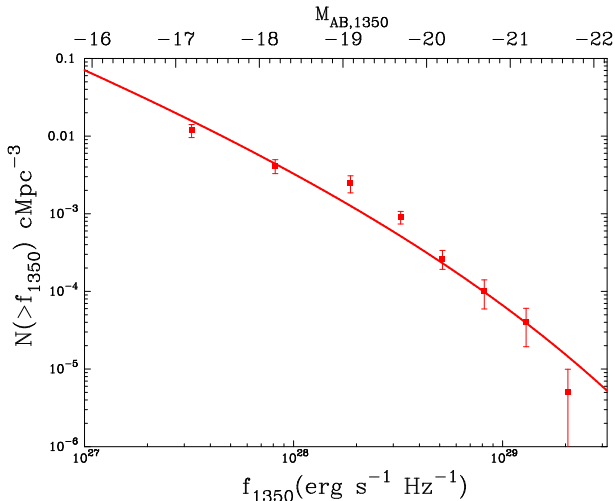


**Figure 7.** Comparison of the best-fit population III model (shown in Figure 5) with the UV-LF constructed by Bouwens et al. (2006) using  $\sim 300$  LBGs in the Hubble Deep Fields. This good agreement is likely a coincidence since in our model all LBGs have an observed  $EW \gtrsim 30 \text{ \AA}$ , while the observations show that  $\sim 40\%$  of all LBGs are not detected in  $Ly\alpha$  ( $EW \lesssim 6 \text{ \AA}$ ). This overlap could possibly be (partly) due to a lower dust content of LAEs relative to their  $Ly\alpha$  quiet counterparts (see text).

cloud medium of negligible  $Ly\alpha$  opacity. Under such conditions, the continuum photons can suffer more attenuation than  $Ly\alpha$  photons which bounce from cloud to cloud and mainly propagate through the hot, transparent inter-cloud medium (Neufeld 1991; Hansen & Oh 2006). This attenuation of continuum leads to a large EW. We point out that in this scenario, large EW LAEs are not intrinsically brighter in  $Ly\alpha$ . At fixed  $Ly\alpha$  flux, one is therefore equally likely to detect a low EW LAE. In other words, to produce the observed EW distribution one requires preferential destruction of continuum flux by dust in  $\sim 50\%$  of the galaxies. Currently there is no evidence that this mechanism is at work even in one galaxy. Furthermore, the rest-frame UV colors of galaxies in the Hubble Ultra Deep Field imply that dust in high-redshift galaxies suppresses the continuum flux by only a factor of  $\sim 1.4$  (Bouwens et al. 2006). The maximum boost of the EW in a multi-phase ISM is therefore 1.4, which is not nearly enough to produce intrinsic equivalent widths of  $EW \sim 600 - 800 \text{ \AA}$ . In summary, the only model able to simultaneously explain all observations calls for a short burst of very massive star formation.

### 6.3 Comparison with the LBG Population

In § 5.1 we have shown that the observed EW distributions of  $Ly\alpha$  selected and i-drop galaxies and their differences can be reproduced qualitatively with our population III model. However, in our model all high-redshift galaxies have an observed EW of at least  $\mathcal{T}_\alpha \times EW_{II} \sim 30 \text{ \AA}$ , whereas many i-drop galaxies are not detected in  $Ly\alpha$ . Kashikawa et al. (2006) show that the UV-LFs of LAEs at  $z = 6.5$  and  $z = 5.7$  overlap with that constructed by Bouwens et al. (2006) from a sample of  $\sim 300$   $z = 6$  LBGs discovered in the Hubble Deep Fields. Naively, this overlap implies that

LBGs and LAEs are the same population and therefore that all LBGs should be detected by  $Ly\alpha$  surveys. Since  $Ly\alpha$  surveys only detect galaxies with  $EW \gtrsim 20 \text{ \AA}$ , this suggests all LBGs should have a  $Ly\alpha$   $EW \gtrsim 20 \text{ \AA}$  contrary to observation. To illustrate this point further, we have taken the best-fit population III model shown in Figure 5 and compared the model predictions for the rest-frame UV-LF with that of Bouwens et al. (2006) in Figure 7. Clearly, our best-fit population III model fits the data well. However, Stanway et al. (2007) found  $\sim 40\%$  of i-drop galaxies in the HUDF to have an observed  $EW \lesssim 6 \text{ \AA}$ , and a similar result was presented by Dow-Hygelund et al. (2007).

Two effects may help reconcile these two apparently conflicting sets of observations: (i) Dow-Hygelund et al. (2007) found  $Ly\alpha$  emitting LBGs to be systematically smaller. That is, for a fixed angular size, the  $z_{850}$ -band flux of LAEs is systematically higher with  $\Delta z_{850} \sim -1$ . If we assume that the angular scale of a galaxy is determined by the mass of its host halo, then this implies that for a fixed mass the  $z_{850}$ -band flux of LAEs is systematically higher, and (ii) only a fraction of LBGs are LAEs. The drop-out technique used to select high redshift galaxies is known to introduce a bias against strong LAEs, as a strong  $Ly\alpha$  line can affect the broad band colors of high-redshift galaxies. This may cause  $\sim 10 - 46\%$  of large EW LAEs to be missed using the i-drop technique (Dow-Hygelund et al. 2007).

If only a fraction  $f_\alpha$  of all LBGs are detected in  $Ly\alpha$ , then effect (i) would explain why the UV-LF of LAEs lies less than a factor of  $1/f_\alpha$  below the observed UV-LF of the general population of LBGs. This is because a more abundant lower mass halo is required to produce the same UV-flux in LAEs, which would shift the LF upwards. In addition, effect (ii) may reduce this difference even further. It follows that these two effects combined may cause the LFs to overlap. Thus the overlap of the UV and  $Ly\alpha$  selected UV-LFs appears to be a coincidence, and not evidence of their being the same population of galaxies. This implies that our model is valid for  $Ly\alpha$  selected galaxies, but not the high-redshift population as a whole and explains the lack of very low EWs in UV selected samples discussed in § 5.1.

The reason why LAEs may be brighter in the UV for a fixed halo mass is unclear. It is possibly related to dust content. Bouwens et al. (2006) found the average amount of UV extinction to be 0.4 mag in the total sample of  $z = 6$  LBGs. This value is close to the average excess  $z_{850}$ -band flux detected from LAEs for a given angular scale (Dow-Hygelund et al. 2007). If LAEs contain less (or no) dust, then this would explain why they are brighter in the UV and thus why they appear more compact. The possibility that ‘ $Ly\alpha$  quiet’ LBG contain more dust than their  $Ly\alpha$  emitting counterparts is not very surprising, as a low dust abundance has the potential to eliminate the  $Ly\alpha$  line. Thus LAEs could be high redshift galaxies with a lower dust content.

Shimasaku et al. (2006) and Ando et al. (2006) found that luminous LBGs,  $M_{UV} \lesssim -21.0$ , typically do not contain large EW  $Ly\alpha$  emission lines. This deficiency of large EW LAEs among UV-bright sources is not expected in our model, and may reflect that UV-bright sources are more massive, mature, galaxies that cannot go through a population-III phase anymore. It should be pointed out though that the absence of large EW LAEs among galax-

ies with  $M_{UV} \lesssim -21.0$  in the survey of Shimasaku et al. (2006) is consistent with our model: The observed number density of sources with  $M_{UV} \lesssim -21.0$  is  $\sim 5 \times 10^{-5}$   $\text{cMpc}^{-3}$  (see Fig 1). In our best-fit pop-III model (shown in Fig 5), a fraction  $f_{III} \sim 0.08$  of these galaxies would be in the bright phase. This translates to a number density of large EW LAEs of  $\sim 4 \times 10^{-6}$   $\text{cMpc}^{-3}$ . Given the survey volume of  $\sim 2 \times 10^5$   $\text{cMpc}^3$ , the expected number of large EW LAEs with  $M_{UV} \lesssim -21.0$  is  $\sim 0.8$ , and the absence of large EW LAE among UV bright sources is thus not surprising.

#### 6.4 Clustering Properties of the LAEs

In our model large EW LAEs are less massive by a factor of  $EW_{III}/EW_{II} \sim 4$  at fixed  $\text{Ly}\alpha$  luminosity. Since clustering of dark matter halos increases with mass, it follows that our model predicts large EW LAEs to be clustered less than their low EW counterparts (at a fixed  $\text{Ly}\alpha$  luminosity). The clustering of LAEs is typically quantified by their angular correlation function (ACF),  $w(\theta)$ , which gives the excess (over random) probability of finding a pair of LAEs separated by an angle  $\theta$  on the sky. The ACF depends on the square of the bias parameter ( $w(\theta) \propto b^2(m)$ ), which for galaxies in the population II phase is  $\sim 1.24 - 1.4$  times larger than for galaxies in the population III phase, for the mass range of interest. This implies that the clustering of low EW LAEs at fixed  $\text{Ly}\alpha$  luminosity is enhanced by a factor of  $\sim 1.5 - 2.0$ . Existing determinations of the ACF of LAEs by Shimasaku et al. (2006) and Kashikawa et al. (2006) are still too uncertain to test this prediction.

## 7 CONCLUSIONS

Observations of high redshift  $\text{Ly}\alpha$  emitting galaxies (LAEs) have shown the typical equivalent width (EW) of the  $\text{Ly}\alpha$  line to increase dramatically with redshift, with a significant fraction of the galaxies lying at  $z \geq 5.7$  having an  $EW \gtrsim 100 \text{ \AA}$ . Recent calculations by Dijkstra et al. (2007) show that the IGM at  $z \geq 4.5$  transmits only 10 – 30% of the  $\text{Ly}\alpha$  photons emitted by galaxies. In this paper we have investigated the transmission using a model that reproduces the observed  $\text{Ly}\alpha$  and UV LFs. This model results in an empirically determined transmission of  $\mathcal{T}_\alpha \sim 0.30(\mathcal{L}_{\alpha,42}/2.0)^{-1}$ , where  $\mathcal{L}_{\alpha,42}$  denotes the  $\text{Ly}\alpha$  luminosity per unit star formation rate (in  $M_\odot \text{ yr}^{-1}$ )  $\mathcal{L}_\alpha$  in units of  $10^{42} \text{ erg s}^{-1}$  (§ 3). This value is in good agreement with earlier theoretical results.

If only  $\sim 30\%$  of all  $\text{Ly}\alpha$  that was emitted by high redshift galaxies reaches the observer, then this implies that the intrinsic EWs are systematically (much) larger than observed in many cases. To investigate the origin of these very high EWs, we have developed semi-analytic models for the  $\text{Ly}\alpha$  and UV luminosity functions and the distribution of equivalent widths. In this model  $\text{Ly}\alpha$  emitters undergo a burst of very massive star formation that results in a large intrinsic EW, followed by a phase of population-II star formation that produces a lower EW<sup>3</sup>. This model is referred

to as the ‘population III model’ and is an extension of the idea originally described by Malhotra & Rhoads (2002), who proposed large EW  $\text{Ly}\alpha$  emitters to be young galaxies.

The population III model in which the  $\text{Ly}\alpha$  equivalent width is  $EW_{III} \sim 650(\mathcal{L}_{\alpha,42}/2.0) \text{ \AA}$  for  $\lesssim 50$  Myr, is able to simultaneously describe the following eight properties of the high redshift galaxy population: i-iv) the UV and  $\text{Ly}\alpha$  luminosity functions of LAEs at  $z=5.7$  and 6.5, v-vi) the mean and variance of the EW distribution of  $\text{Ly}\alpha$  selected galaxies at  $z=5.7$ , vii) the EW distribution of UV- selected galaxies at  $z\sim 6$  (§ 5), and viii) the observed correlation of stellar age and mass with EW (§ 6.1). Our modeling suggests that the anomalously large intrinsic equivalent widths observed in about half of the high redshift  $\text{Ly}\alpha$  emitters require a burst of very massive star formation lasting no more than a few to ten percent of the galaxies star forming lifetime. This very massive star formation may indicate the presence of population-III star formation in a large number of high-redshift LAEs. The model parameters for the best-fit model are physically plausible where not previously known (e.g. those related to the efficiency and duration of star formation), and agree with estimates where those have been calculated directly (e.g. the IGM transmission,  $EW_{III}$ , and  $f_{III}$ ).

In addition, we argued that the observed overlap of the UV-LFs of LAEs with that of  $z\sim 6$  LBGs appears to be at odds the observed  $\text{Ly}\alpha$  detection rate in high-redshift LBGs, suggesting that LAEs and LBGs are not the same population. A lower dust content of LAEs relative to their ‘ $\text{Ly}\alpha$  quiet’ counterparts would partly remedy this discrepancy, and could also explain why LAEs appear to be typically more compact (§ 6.3).

Semi-analytic modeling of the coupled reionisation and star formation histories of the universe suggests that population III star formation could still occur after the bulk of reionisation had been completed (Scannapieco et al. 2003; Schneider et al. 2006; Wyithe & Cen 2007). The observation of anomalously large EWs in  $\text{Ly}\alpha$  emitting galaxies at high redshift may therefore provide observational evidence for such a scenario. In the future, the He 1640  $\text{\AA}$  may be used as a complementary probe (e.g. Tumlinson et al. 2001, 2003). The EW of this line is smaller by a factor of  $\gtrsim 20$  for population III (Schaerer 2003). However, the He 1640  $\text{\AA}$  will not be subject to a small transmission of  $\sim 10 - 30\%$ , making it accessible to the next generation of space telescopes. On the other hand, it may also be possible to observe the He 1640  $\text{\AA}$  in a composite spectra of  $z = 6$  LBGs. Indeed, the He 1640  $\text{\AA}$  line has already been observed in the composite spectrum of  $z = 3$  LBGs (Shapley et al. 2003), which led Jimenez & Haiman (2006) to argue for population III star formation at redshifts as low as  $z = 3 - 4$ . If population III star formation was more widespread at higher redshifts, as predicted by our model, then the composite spectrum

their lifetimes. Our model does not specify when this population-III phase occurs. Hypothetically, the population III phase could occur at an arbitrary moment in the galaxies’ lifetime when it is triggered by a merger of a regular star forming galaxy and a dark matter halo containing gas of primordial composition. Note however that such a model would probably have difficulties explaining the apparent observed correlation between  $\text{Ly}\alpha$  EW and the age of a stellar population (§ 6.1).

<sup>3</sup> Technically, the model discussed in § 5 only specifies that galaxies go through a ‘population-III phase for a fraction  $f_{III} \sim 0.1$  of

of LBGs at higher redshifts should exhibit an increasingly prominent He 1640 Å line. In particular, this line should be most prominent in the subset of LBGs that have large EW Ly $\alpha$  emission lines.

**Acknowledgments** JSBW and MD thank the Australian Research Council for support. We thank Avi Loeb for useful discussions, and an anonymous referee for a helpful report that improved the content of this paper.

## REFERENCES

- Ahn, S.-H., Lee, H.-W., & Lee, H. M. 2003, *MNRAS*, 340, 863
- Ahn, S.-H. 2004, *ApJL*, 601, L25
- Ando, M., Ohta, K., Iwata, I., Akiyama, M., Aoki, K., & Tamura, N. 2006, *ApJL*, 645, L9
- Barkana, R. 2004, *MNRAS*, 347, 59
- Bouwens, R. J., Illingworth, G. D., Blakeslee, J. P., & Franx, M. 2006, *ApJ*, 653, 53
- Bromm, V., Kudritzki, R. P., & Loeb, A. 2001, *ApJ*, 552, 464
- Charlot, S., & Fall, S. M. 1993, *ApJ*, 415, 580
- Dawson, S., et al. 2004, *ApJ*, 617, 707
- Dijkstra, M., Lidz, A., & Wyithe, J. S. B. 2007, *MNRAS*, 377, 1175
- Dijkstra, M., Wyithe, J.S.B., & Haiman, Z., 2007b, *MNRAS* Imm in press, astro-ph/0611195
- Dow-Hygelund, C. C., et al. 2007, *ApJ*, 660, 47
- Ferrara, A., & Ricotti, M. 2006, *MNRAS*, 373, 571
- Finkelstein, S. L., Rhoads, J. E., Malhotra, S., Pirzkal, N., & Wang, J. 2007, *ApJ*, 660, 1023
- Gawiser, E., et al. 2006, *ApJL*, 642, L13
- Hansen, M., & Oh, S. P. 2006, *MNRAS*, 367, 979
- Hu, E. M., & McMahon, R. G. 1996, *Nature*, 382, 231
- Hu, E. M., Cowie, L. L., McMahon, R. G., Capak, P., Iwamura, F., Kneib, J.-P., Maihara, T., & Motohara, K. 2002, *ApJL*, 568, L75
- Hu, E. M., Cowie, L. L., Capak, P., McMahon, R. G., Hayashino, T., & Komiyama, Y. 2004, *AJ*, 127, 563
- Iye, M., et al. 2006, *Nature*, 443, 186
- Jimenez, R., & Haiman, Z. 2006, *Nature*, 440, 501
- Kashikawa, N., et al. 2006, *ApJ*, 648, 7
- Kennicutt, R. C., Jr. 1998, *ARA&A*, 36, 189
- Kodaira, K., et al. 2003, *PASJ*, 55, L17
- Kunth, D., Mas-Hesse, J. M., Terlevich, E., Terlevich, R., Lequeux, J., & Fall, S. M. 1998, *A&A*, 334, 11
- Lai, K., Huang, J.-S., Fazio, G., Cowie, L. L., Hu, E. M., & Kakazu, Y. 2007, *ApJ*, 655, 704
- Loeb, A., Barkana, R., & Hernquist, L. 2005, *ApJ*, 620, 553
- Malhotra, S., & Rhoads, J. E. 2002, *ApJL*, 565, L71
- Malhotra, S., Wang, J. X., Rhoads, J. E., Heckman, T. M., & Norman, C. A. 2003, *ApJL*, 585, L25
- Mao, J., Lapi, A., Granato, G. L., de Zotti, G., & Danese, L. 2007, Submitted to *ApJ*, astro-ph/0611799
- Nagao, T., et al. 2007, *ArXiv Astrophysics e-prints*, arXiv:astro-ph/0702377
- Neufeld, D. A. 1991, *ApJL*, 370, L85
- Partridge, R. B., & Peebles, P. J. E. 1967, *ApJ*, 147, 868
- Pirzkal, N., Malhotra, S., Rhoads, J. E., & Xu, C. 2006, *ArXiv Astrophysics e-prints*, arXiv:astro-ph/0612513
- Press, W. H., & Schechter, P. 1974, *ApJ*, 187, 425
- Rhoads, J. E., Malhotra, S., Dey, A., Stern, D., Spinrad, H., & Januzzi, B. T. 2000, *ApJL*, 545, L85
- Scannapieco, E., Schneider, R., & Ferrara, A. 2003, *ApJ*, 589, 35
- Schaerer, D. 2003, *A&A*, 397, 527
- Schaerer, D., & Pelló, R. 2005, *MNRAS*, 362, 1054
- Schneider, R., Salvaterra, R., Ferrara, A., & Ciardi, B. 2006, *MNRAS*, 369, 825
- Shapley, A. E., Steidel, C. C., Pettini, M., & Adelberger, K. L. 2003, *ApJ*, 588, 65
- Sheth, R. K., Mo, H. J., & Tormen, G. 2001, *MNRAS*, 323, 1
- Shimasaku, K., et al. 2006, *PASJ*, 58, 313
- Spergel, D. N., et al. 2007, *ApJS*, 170, 377
- Stanway, E. R., et al. 2004, *ApJL*, 604, L13
- Stanway, E. R., McMahon, R. G., & Bunker, A. J. 2005, *MNRAS*, 359, 1184
- Stanway, E. R., et al. 2007, *MNRAS*, 376, 727
- Stark, D. P., Loeb, A., & Ellis, R. S. 2007, *ArXiv Astrophysics e-prints*, arXiv:astro-ph/0701882
- Taniguchi, Y., et al. 2005, *PASJ*, 57, 165
- Tapken, C., Appenzeller, I., Noll, S., Richling, S., Heidt, J., Meinköhn, E., & Mehlert, D. 2007, *A&A*, 467, 63
- Tumlinson, J., Giroux, M. L., & Shull, J. M. 2001, *ApJL*, 550, L1
- Tumlinson, J., Shull, J. M., & Venkatesan, A. 2003, *ApJ*, 584, 608
- Verhamme, A., Schaerer, D., & Maselli, A. 2006, *A&A*, 460, 397
- Wang, J. X., et al. 2004, *ApJL*, 608, L21
- Westra, E., et al. 2006, *A&A*, 455, 61
- Wyithe, J. S. B., & Cen, R. 2007, *ApJ*, 659, 890
- Wyithe, J. S. B., & Loeb, A. 2007, *MNRAS*, 375, 1034